# Arbitrary focusing lens by holographic metasurface

**Rongzhen Li,[1] Zhongyi Guo,[1,2,*] Wei Wang,[2,3] Jingran Zhang,[1] Keya Zhou,[3] Jianlong Liu,[3] Shiliang Qu,[2] Shutian Liu,[3] and Jun Gao[1]**

[1]*School of Computer and Information, Hefei University of Technology, Hefei 230009, China*
[2]*Department of Optoelectronics Science, Harbin Institute of Technology at Weihai, Weihai 264209, China*
[3]*Department of Physics, Harbin Institute of Technology, Harbin 150001, China*
**Corresponding author: guozhongyi@hfut.edu.cn*

Received May 6, 2015; revised July 21, 2015; accepted July 24, 2015;
posted August 5, 2015 (Doc. ID 242674); published August 31, 2015

In this paper, an ultrathin metalens has been proposed based on a holographic metasurface that consists of elongated apertures in 40 nm gold film, which exhibit intriguing properties such as on- and off-axis focusing and also can concentrate light into multiple, discrete spots for circularly polarized incident lights. First, the spatial transmission phase distributions of the designed metalens with arbitrary focusing can be obtained by computer-generated holography. Then, the discrete phase distributions can be continuously encoded by subwavelength nanoapertures with spatially varying orientations in gold film. The simulation results show that our designed metalens can work efficiently for different types of focusing. Finally, our metasurface shows superior broadband characteristics between 670 and 810 nm, and the corresponding focal lengths of the designed lenses also can be efficiently modulated with the incident lights at different wavelengths. 

*OCIS codes:* (160.3918) Metamaterials; (230.0230) Optical devices; (060.5060) Phase modulation; (140.4780) Optical resonators.
http://dx.doi.org/10.1364/PRJ.3.000252

## 1. INTRODUCTION

With the advent of the metasurface, wide applications have been proposed, such as creating optical vortex beams [1], coupling propagating waves to surface waves [2], creating ultrathin circular polarization analyzers [3], fabricating phase holograms [4], designing continuous metasurfaces [5,6], and so forth. Among all the applications of metasurfaces, one intriguing development is the plasmonic metalens for concentrating light, with miniature and ultrathin characteristics, which has recently attracted strong interest. As we know, the convergence of an optical beam in a traditional, refraction-based lens depends on the phase modulation via gradual phase changes accumulated along the optical paths, which is limited by the refractive index of a dielectric. Fabrication challenges are also paramount, as it is difficult to make lenses with a large aperture and a short focal length. By using the Fresnel lens design, the mass and volume of material can be reduced, but the thickness of the lens is still on the wavelength scale.

However, advances in the area of metasurfaces have opened up a new era for building miniature planar lenses, which are known as the metalens, because an abrupt phase change over the scale of the wavelength has been recently discovered by using a metasurface. A plethora of lenses based on a metasurface have been recently developed with the ability to focus light in 2D [7–9] or 3D space [10–13] following the equal optical path principle [11,12]:

$$\varphi(x,y) = 2n\pi + \frac{2\pi}{\lambda}\left(\sqrt{f^2 + (x^2 + y^2)} - f\right), \qquad (1)$$

where $\varphi(x,y)$ is the phase shift imposed in every point on the flat lens, $n$ is an arbitrary integer, $\lambda$ is the incident wavelength in free space, and $f$ is the given focal length. Notably, the phase of a metalens designed by this method is discrete. Especially, for 2D focusing, the metalens, such as the cylindrical lens previously demonstrated, only manipulated the light along one direction owing to one-directional phase variation, resulting in image distortion of an arbitrary object due to the different magnifications along two directions. Although 3D focusing has been proposed, which can resolve this problem, these designs suffer from only a single focusing spot or the spot that resides in the optical axis of the lens. Furthermore, a dual-polarity plasmonic metalens [8,14] at the visible and near-infrared range also have been proposed, which demonstrate the positive lens for the right circularly polarized (RCP) incident light and the negative lens for the left circularly polarized (LCP) incident light and vice versa. Nevertheless, these designs also focus incident light into a single spot. Thus, it remains a challenge to focus the light into arbitrary spots or multiple spots by metasurface.

In this paper, we have proposed an ultrathin planar metalens constructed by nanoapertures in gold film. The metalenses not only exhibit on-axis focusing but off-axis focusing and multiple spot focusing for normal incidence, which are designed based on holographic metasurface [15] at the wavelength of 740 nm. The designing approach of our metalens combines the computer-generated holography (CGH) method and the metasurface: an appropriate transmitting phase distributions of the lens with different focusing characters can be obtained by CGH; then, the obtained phase distributions can be continuously expressed and modulated by subwavelength nanoapertures with spatially varying orientations in gold film. Moreover, the robustness of our metasurface also has been numerically demonstrated.

 

## 2. DESIGNS

For our demonstration, the holographic metasurface contains $33 \times 33$ pixels with a lattice constant of 300 nm, which represent unique optical focusing profiles. Furthermore, each pixel consists of an aperture with a determined orientation angle of $\theta$ along the $x$ direction, which is fabricated in the gold film with the thickness of 40 nm, and the aperture dimension is 150 nm × 75 nm. The transmitted lights for the circularly polarized light incidence to the aperture can be decomposed into two circular polarization components, with one component possessing the same helicity as the incident light and a phase that does not depend on the orientation of the aperture, and the other with opposite helicity (cross polarization) to the incident light and a phase (Pancharatnam–Berry phase) [16,17] that is twice the orientation angle of the aperture. Therefore, an arbitrary phase simply can be achieved by controlling the orientation angles of the apertures, which greatly eases the encoding procedure of phase-only metalens. Here we have assumed that the phase deviations from the coupling effects of the neighboring nano-aperture is negligible [18]. Particularly, such phase discontinuity is geometric in nature and does not rely on the incident wavelength, which leads to the robustness of our metalens. The schematic of the metalens structure and focusing procedure are illustrated in Fig. 1. The metalens will provide a desired phase to obtain the corresponding focusing profiles.

In order to realize various focusing patterns (on-/off-axis and multiple focusing), the corresponding phase distributions of the transmission lights can be determined by the CGH method [19] by using MATLAB. After obtaining the concrete phase patterns, the corresponding holographic metasurfaces can be achieved by using the orientational aperture array, which is modulated according to the relationship between the phase and aperture orientation. Each pixel of the holographic metasurface only contains a single subwavelength nanoaperture whose orientation encodes the desired local phase profile for an incident LCP light. It should be noted that the pixel size along each direction is less than half of the wavelength, ensuring that the hologram pattern is sampled at least at twice the maximum spatial frequency in either direction, thereby satisfying the Shannon–Nyquist sampling theorem [18].

The holographic metasurfaces are designed at the wavelength of 740 nm for all of the metalenses here. The simulated result in Fig. 2 shows the amplitude for the transmitting

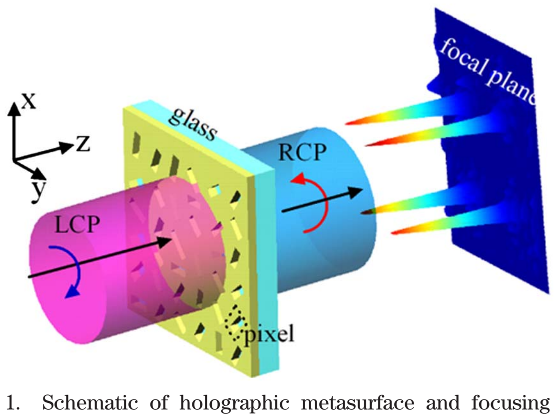


Fig. 1. Schematic of holographic metasurface and focusing procedure. For LCP light incidence, the transmitting cross-polarized light (RCP) is focused into various points.

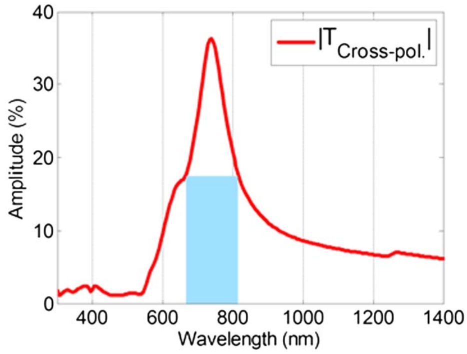


Fig. 2. Illustration of efficiency for one-pixel cell structure by numerical simulation. Amplitude as a function of wavelength.

cross-polarization (RCP) light for LCP normal incidence, and the transmitted amplitude can reach to 36% for the incident light with the wavelength of 740 nm. Although the efficiency goes down fast around 740 nm, the focusing performance is still acceptable for the transmitting metalens composed of metasurface structures. We define the wavelength range over the shadowed region (670–810 nm), which corresponds to the FWHM of the amplitude's transmitted efficiency. Furthermore, the broadband characteristics of the designed metalens have also been investigated in detail in the following simulations. All of the simulation results are obtained by the FDTD method.

## 3. RESULTS AND DISCUSSION

As depicted in Fig. 3, the first holographic metasurface is designed to focus incident light into a single spot along the optical axis for LCP normal incidence at the wavelength of 740 nm. Figure 3(a) demonstrates that the designed metalens based on the hologram method can be exploited for creating a unique 3D optical profile. The intensity here is defined as $|E_{\text{cross}}|^2$. It is a cross-polarized component that contributes to the focusing spot, which agrees well with our previous analysis. The desired phase pattern for the on-axis focusing, which can be obtained by CGH method, is illustrated in Fig. 3(b). The encoded aperture distribution can be obtained according to the corresponding phase pattern [Fig. 3(b)], as depicted in Fig. 3(c). Furthermore, the phase pattern is similar to the one achieved by lattice evolution algorithm (LEA) [20] or derived from the equal optical path principle, which also can verify our approach to be feasible.

As described earlier, a distinct advantage of our holographic metasurface, beyond previous designs using the equal optical path principle, is the ability to simply produce a large

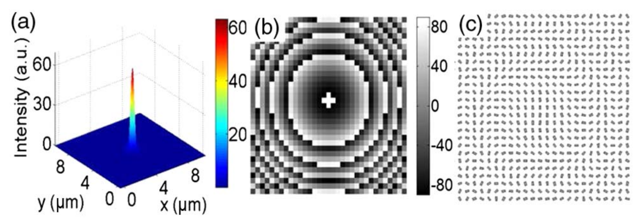


Fig. 3. Transmitted RCP light is focused into a single spot. (a) Intensity distributions in the focal plane for LCP incidence at the wavelength of 740 nm. (b) Phase pattern of single spot. (c) Encoded aperture distribution according to the phase pattern in (b).

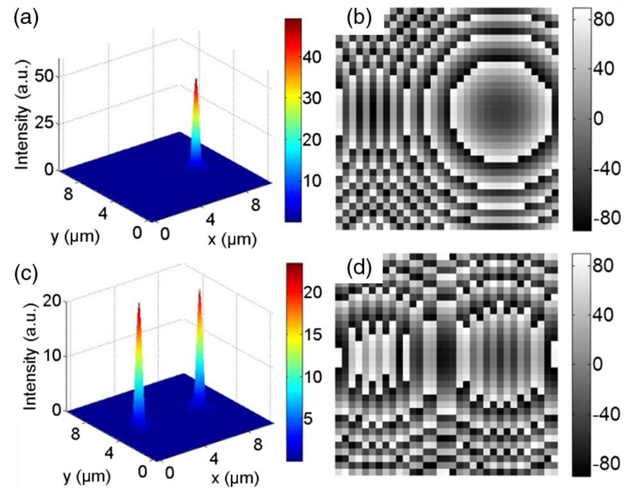


Fig. 4. Focusing performance of the holographic metasurface. (a) and (c) Intensity distributions of the single and two off-axis focusing in the focal planes, respectively. (b) and (d) Corresponding phase patterns.

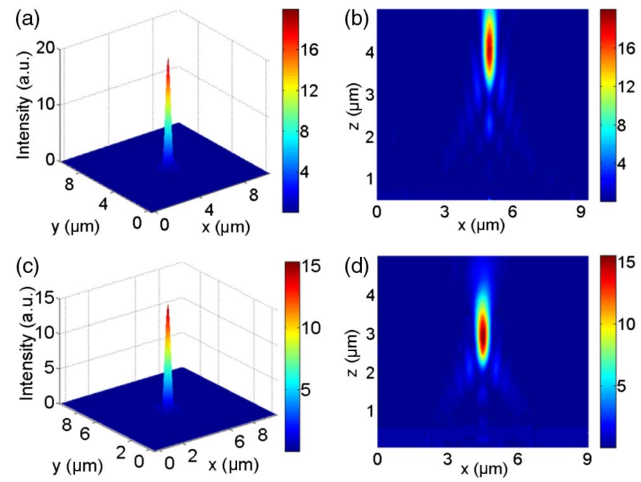


Fig. 6. (a) and (c) Intensity distribution of single focusing spot at the focal plane for the incidence wavelength of 670 and 810 nm. (b) and (d) Corresponding lateral view in *xoz* plane.

range of different 3D optical profiles. As a proof-of-concept, we design various metalenses that can focus light into a single off-axis point or multiple points, which are distinct from previous works based on metasurfaces [10]. The simulated results on the single off-axis focusing can be observed in Fig. 4(a), where the intensity distribution is shown in 3D space in the focal plane. The corresponding phase pattern for off-axis focusing is depicted in Fig. 4(b). It is expected that the focusing spot can be located in an arbitrary position of 3D space by using a proper phase pattern and encoding with the metasurface structural array, which have a promising application prospect in the integrated optics. Furthermore, the two off-axis focusing spots also have been implemented and realized based on holographic metasurfaces, as shown in Figs. 4(c) and 4(d).

To demonstrate the multiple focusing abilities of the metalens, the holographic metasurfaces are designed to concentrate the incident beam into four spaced spots and eight spaced spots, respectively, which exhibit strong focusing capability compared with those of the previous works. The intensity distribution of four focusing spots is located in the symmetric position with nearly the same intensity, as shown in Fig. 5(a), for LCP normal incidence. Furthermore, Fig. 5(b) shows that the designed holographic metasurface can concentrate the incident light to more arbitrary distinct locations (eight spots here). In this case, the eight focusing spots are

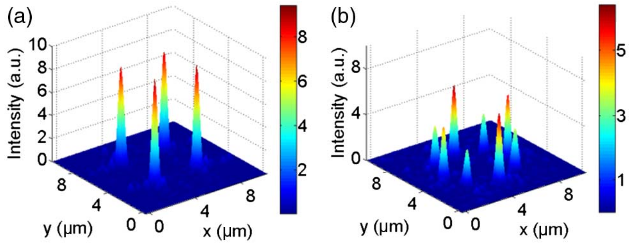


Fig. 5. Multiple spot focusing performance of the holographic metasurface. (a) Intensity distributions of four spots focusing at the focal plane ($z = 4200$ nm). (b) Eight spot focusing performance.

in a circular structure without the central spot. We find that some differences in the intensity distributions of the generated eight focusing spots, which can be attributed to the scale limitation of the simulated region because of the limited computing ability in our group. We can expect a perfect focusing pattern for the more complicated multiple focusing if the simulated region is effectively enlarged. In addition, our holographic metasurfaces for arbitrary focusing are only phase-dependent, whereas the corresponding amplitudes are not controlled and modulated accordingly, which may also introduce some errors. Although the intensity distributions of the generated multiple focusing spots have some blemishes, we also can imagine that the arbitrary focusing ability of the designed holographic metasurface should have great potential in various applications in integrated optics, such as orbital angular momentum-based optical communication systems, special Dammann gratings, and so forth.

To further demonstrate the robustness of our metalens (for investigating the broadband characteristics), various wavelengths (670–810 nm) of the LCP lights are vertically incident to the holographic metasurface designed at 740 nm for single-spot focusing without loss of generality (easy to observe the various focal lengths). As depicted in Figs. 6(a) and 6(c), under normal incidence of LCP light, a single focusing spot is observed for the wavelengths of 670 and 810 nm, respectively, and the lateral view of intensity distributions in the *xoz* plane are shown in Figs. 6(b) and 6(d), respectively. The focal lengths are 4200 nm for the wavelength of 670 and 2900 nm for the wavelength of 810 nm respectively, as illustrated in Figs. 6(b) and 6(d), which is different for the focal length of 4000 nm when the incident wavelength is 740 nm. It is foreseeable that the focal length will decrease with gradually increasing the incident wavelength. Furthermore, the focal length can be modulated by changing the incident wavelengths. On the other hand, the simulation results also demonstrate the superior broadband characteristics of our metasurface in the range of 670–810 nm, which can be attributed to the fact that the phase control by the directions of the elongated apertures is geometric in nature and does not rely on the incident wavelengths.

## 4. CONCLUSION

In summary, in this work a new type of planar holographic metasurface designed for simple and sophisticated focusing is proposed and numerically investigated at the wavelength of 740 nm. The approach combines the CGH method with a Pancharatnam–Berry phase, which is simple to achieve in the desired phase pattern and to realize the continuous encoding phase by the directions of the elongated apertures. The simulation results demonstrate that our approach is accurate and credible for designing metalenses. Different types of focusing behaviors, including single or multiple on-/off-axis focusing, have been realized in high quality. Furthermore, our metalens show superior broadband characteristics, and the focal length of the designed metalens also can be modulated by changing the incident wavelength.

## Acknowledgment

The authors gratefully acknowledge the financial supports for this work from the Fundamental Research Funds for the Central Universities (2015HGCH0010), and the Foundation of Hefei University of Technology of China (HFUT. 407-037026).

## REFERENCES


1. P. Genevet, N. Yu, F. Aieta, J. Lin, M. Kats, R. Blanchard, M. Scully, Z. Gaburro, and F. Capasso, "Ultra-thin plasmonic optical vortex plate based on phase discontinuities," Appl. Phys. Lett. **100**, 013101 (2012).
2. S. Sun, Q. He, S. Xiao, Q. Xu, X. Li, and L. Zhou, "Gradient-index meta-surfaces as a bridge linking propagating waves and surface waves," Nat. Mater. **11**, 426–431 (2012).
3. R. Z. Li, Z. Y. Guo, W. Wang, J. R. Zhang, A. J. Zhang, J. L. Liu, S. L. Qu, and J. Gao, "Ultra-thin circular polarization analyzer based on the metal rectangular split-ring resonators," Opt. Express **22**, 27968–27975 (2014).
4. X. Ni, A. V. Kildishev, and V. M. Shalaev, "Metasurface holograms for visible light," Nat. Commun. **4**, 2807 (2013).
5. Z. Li, L. Huang, K. Lu, Y. Sun, and L. Min, "Continuous metasurface for high-performance anomalous reflection," Appl. Phys. Express **7**, 112001 (2014).
6. L. Zhang, J. Hao, M. Qiu, S. Zouhdi, J. K. W. Yang, and C. W. Qiu, "Anomalous behavior of nearly-entire visible band manipulated with degenerated image dipole array," Nanoscale **6**, 12303–12309 (2014).
7. W. Wang, Z. Y. Guo, R. Z. Li, J. R. Zhang, Y. Liu, X. Wang, and S. L. Qu, "Ultra-thin, planar, broadband, dual-polarity plasmonic metalens," Photon. Res. **3**, 68–71 (2015).
8. D. Hu, X. Wang, S. Feng, J. Ye, W. Sun, Q. Kan, J. K. Peter, and Y. Zhang, "Ultrathin terahertz planar elements," Adv. Opt. Mater. **1**, 186–191 (2013).
9. A. Pors, M. G. Nielsen, R. L. Eriksen, and S. I. Bozhevolnyi, "Broadband focusing flat mirrors based on plasmonic gradient metasurfaces," Nano Lett. **13**, 829–834 (2013).
10. F. Aieta, P. Genevet, M. A. Kats, N. Yu, R. Blanchard, Z. Gaburro, and F. Capasso, "Aberration-free ultrathin flat lenses and axicons at telecom wavelengths based on plasmonic metasurfaces," Nano Lett. **12**, 4932–4936 (2012).
11. X. Ni, S. Ishii, A. V. Kildishev, and V. M. Shalaev, "Ultra-thin, planar, Babinet-inverted plasmonic metalenses," Light Sci. Appl. **2**, e72 (2013).
12. X. Li, S. Xiao, B. Cai, Q. He, T. J. Cui, and L. Zhou, "Flat metasurfaces to focus electromagnetic waves in reflection geometry," Opt. Lett. **37**, 4940–4942 (2012).
13. D. Lin, P. Fan, E. Hasman, and M. L. Brongersma, "Dielectric gradient metasurface optical elements," Science **345**, 298–302 (2014).
14. X. Chen, L. Huang, H. Mühlenbernd, G. Li, B. Bai, Q. Tan, F. Guo, W. Cheng, Z. Thomas, and S. Zhang, "Reversible three-dimensional focusing of visible light with ultrathin plasmonic flat lens," Adv. Opt. Mater. **1**, 517–521 (2013).
15. S. A. Kuznetsov, M. A. Astafev, M. Beruete, and M. Navarro-Cía, "Planar holographic metasurfaces for terahertz focusing," Sci. Rep. **5**, 7738 (2015).
16. E. Hasman, V. Kleiner, G. Biener, and A. Niv, "Polarization dependent focusing lens by use of quantized Pancharatnam-Berry phase diffractive optics," Appl. Phys. Lett. **82**, 328–330 (2003).
17. R. Z. Li, Z. Y. Guo, W. Wang, J. R. Zhang, A. J. Zhang, J. L. Liu, S. L. Qu, and J. Gao, "High-efficiency cross polarization converters by plasmonic metasurface," Plasmonics, Doi: 10.1007/s11468-015-9916-3 (in press).
18. G. Zheng, H. Mühlenbernd, M. Kenney, G. Li, T. Zentgraf, and S. Zhang, "Metasurface holograms reaching 80% efficiency," Nat. Nanotechnol. **10**, 308–312 (2015).
19. H. Zhang, Q. Tan, and G. Jin, "Holographic display system of a three-dimensional image with distortion-free magnification and zero-order elimination," Opt. Eng. **51**, 075801 (2012).
20. M. D. Huntington, L. J. Lauhon, and T. W. Odom, "Subwavelength lattice optics by evolutionary design," Nano Lett. **14**, 7195–7200 (2014).